Theor Chim Acta (1992) 81: 255–268

Theoretica Chimica Acta

Ab initio molecular orbital calculations of the infrared spectra of hydrogen-bonded complexes of water, ammonia and hydroxylamine

IX. The hydroxylamine dimers revisited

G. A. Yeo and T. A. Ford

Centre for Molecular Design, Department of Chemistry, University of the Witwatersrand, Johannesburg, Wits 2050, South Africa

Received February 11, 1991/Accepted March 15, 1991

Summary. The geometries of three hydrogen-bonded dimers of hydroxylamine have been optimized, at the MP2 level of theory, using the 6-31G** basis set. These calculations yielded three separate local minima on the dimer potential energy surface. The interaction energies of these three species have been calculated, and corrected for basis set superposition error. The infrared band wavenumbers and intensities have been computed, and the monomer-dimer wavenumber shifts and intensity enhancements rationalized in terms of the types and strengths of hydrogen bonds present. The predicted wavenumbers have been correlated with those measured in a recent matrix isolation spectroscopic study, and an argument for the structure of the preferred dimer has been presented.

Key words: *Ab initio* – Infrared spectra – Hydrogen bonding

1. Introduction

A large volume of literature exists on the structures and properties, particularly the vibrational spectroscopic properties, of the water and ammonia dimers. Reference [1] cites a wealth of references to *ab initio* theoretical studies, and to matrix isolation infrared and Raman, and gas phase molecular beam and microwave spectroscopic studies of these species. It is now generally accepted that the geometries of both these dimers are best described as approximately linearly hydrogen bonded (OH···O and NH···N respectively), but that due to the extreme weakness of the NH···N hydrogen bond in $(NH_3)_2$, the potential energy hypersurface in the region of the global minimum is very flat, and a very small barrier indeed separates the linear from the cyclic hydrogen bonded form [1]. By contrast, similar studies on hydroxylamine are few [2–5].

Hydroxylamine forms an interesting third member of the series containing water and ammonia [6]. It contains structural entities necessary for the formation of hydrogen bonds: a hydroxyl group capable of acting as a proton donor, and a nitrogen atom bearing a lone pair of electrons which can function as a proton acceptor. A first principles prediction of the structure of the hydroxylamine dimer would therefore feature a linear OH···N hydrogen bond [3]. A second plausible structure might involve a cyclic geometry with two OH···N

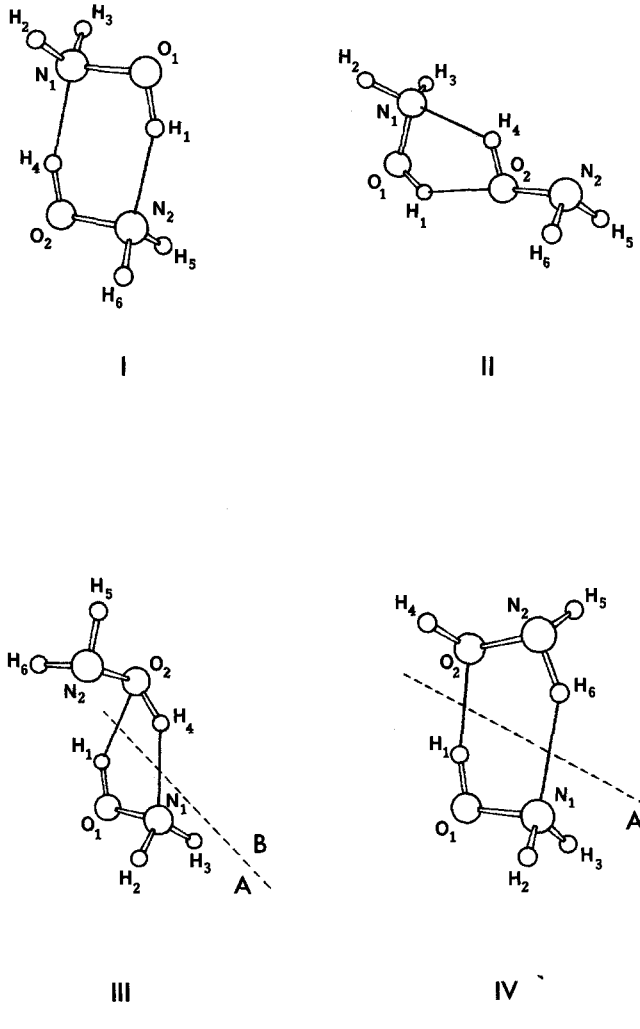

Fig. 1. Four possible structures for the hydroxylamine dimer

bonds in a centrosymmetric arrangement [3]. Other possibilities exist; OH···O, NH···O and NH···N hydrogen bonded structures should not be excluded, although they are considered to be less probable.

The earliest theoretical study of this system appears to be that of Del Bene [2], who used the LCAO-MO-SCF *ab initio* method with a minimal STO-3G [7] basis set to optimize the intermolecular bond lengths and angles of a number of dimers, while maintaining the intramolecular parameters fixed at their STO-3G optimized values. Among the structures considered by Del Bene was the six-membered cyclic geometry, of C_{2h} symmetry, referred to above [2]. In our earlier study of this system [3], at the self-consistent-field level, and employing the 4-31G [8] and 6-31G** [9] basis sets, we also determined the properties of this six-membered cyclic dimer (structure **I**, see Fig. 1), as an analogue of the centrosymmetric cyclic dimers of water and ammonia [1]. As a counterpart of the linear $(H_2O)_2$ and $(NH_3)_2$ dimers, we attempted a geometry optimization of

a linear OH···N bonded dimer of C_s symmetry [3], but found that, on maintaining the C_s symmetry, this dimer relaxed to a five-membered cyclic structure with both OH···N and OH···O hydrogen bonds (structure **II**, Fig. 1). However, at this level of theory, we found that, on carrying out a normal coordinate analysis, the five-membered ring structure yielded two (4-31G) and three (6-31G**) negative eigenvalues, establishing the fact that structure **II** is not a true minimum on the potential energy surface [10]. (In fact, in our preliminary calculation [3], using a less sophisticated procedure, we also found a single negative eigenvalue for the six-membered dimer using the 6-31G** basis set.) In view of our noticeably greater success in computing the properties of the binary complexes $(H_2O)_2$, $(NH_3)_2$ [1], $HOH{\cdot}NH_3$ [6], $HOH{\cdot}NH_2OH$ [11] and $NH_2OH{\cdot}NH_3$ [12] at the second order Møller–Plesset (MP2) level of theory [13], and using the 6-31G** basis set, we decided to repeat our calculations on $(NH_2OH)_2$ [3] using this improved model. We also decided to relax the C_s symmetry constraint of structure **II** to C_1, to investigate whether the appearance of the negative eigenvalues in our earlier calculations could be avoided by allowing the five-membered ring to undergo some puckering, thus freeing the *exo* NH_2 group to move out of the plane of the ring. The final configuration resulting from this procedure is shown as structure **III** in Fig. 1. No negative eigenvalues were found in this case, indicating that structure **III** is a true local potential energy minimum. In addition, a fourth structure, a cyclic dimer containing both OH···O and NH···N hydrogen bonds, and having C_1 symmetry (see structure **IV**, Fig. 1), was obtained as a minimum energy configuration, yielding no negative eigenvalues. A geometry similar to **IV** was also predicted to be a possible hydroxylamine dimer structure by Del Bene [2], using the STO-3G basis set.

Withnall and Andrews, in their study of the infrared spectrum of hydroxylamine and some of its isotopic variants in argon matrices [4], observed five bands which they assigned to hydroxylamine dimers, at 3339, 1469.0, 1155.7, 909.7, and 735.7 cm^{-1}. They did not speculate on the possible structure of the dimer, however. We have also recorded the spectra of hydroxylamine in nitrogen and argon matrices [5], and have been able to make assignments of nine of the observed bands to specific normal modes of the six-membered cyclic dimer (**I**), or alternatively thirteen bands to vibrations of the five-membered cyclic species (**II**). It is the purpose of this paper to extend the list of binary complexes formed from among water, ammonia and hydroxylamine on which we have carried out *ab initio* calculations, at the MP2 level and using the 6-31G** basis set, and to determine which of the proposed models of the hydroxylamine dimer structure that we have considered most closely fits the experimental matrix isolation infrared spectrum [4, 5], thereby establishing the preferred structure of this interesting hydrogen-bonded species.

2. Computational details

The earlier calculations [3] were carried out using the GAUSSIAN-76 [14, 15] and GAUSSIAN-80 [16, 17] computer programs, at the SCF level and using the 4-31G and 6-31G** basis sets. Determination of infrared band wavenumbers and intensities from the computed energies and dipole moment components was a laborious process, and was sometimes subject to error [18–26]. The acquisition of the GAUSSIAN-86 [27] and, later, GAUSSIAN-88 [28] programs, with their automatic normal coordinate analysis features, improved the reliability of these

Table 1. Optimized geometries, dipole moments and rotational constants of the hydroxylamine dimers, calculated at the MP2/6-31G** level of theory

Parameter	Dimer[a]			Monomer[b]
	I	III	IV	
$r(N_1O_1)$/pm	144.4	144.3	144.6	144.9
$r(O_1H_1)$/pm	97.9	97.1	97.3	96.4
$r(N_1H_2)$/pm	101.7	101.6	101.7	101.6
$r(N_1H_3)$/pm	101.7	101.6	101.7	101.6
$r(N_2O_2)$/pm	144.4	145.1	146.0	144.9
$r(O_2H_4)$/pm	97.9	97.8	96.5	96.4
$r(N_2H_5)$/pm	101.7	101.7	101.6	101.6
$r(N_2H_6)$/pm	101.7	101.7	102.1	101.6
$r(N_1\cdots H_4)$/pm	191.4	194.5		
$r(N_1\cdots H_6)$/pm			218.3	
$r(O_2\cdots H_1)$/pm		202.9	188.9	
$N_1O_1H_1$/deg	100.2	100.3	100.9	101.2
$O_1N_1H_2$/deg	104.1	104.1	103.6	103.0
$O_1N_1H_3$/deg	104.1	104.1	103.6	103.0
$H_2N_1H_3$/deg	105.5	106.0	105.1	105.0
$N_2O_2H_4$/deg	100.2	101.4	101.4	101.2
$O_2N_2H_5$/deg	104.1	103.1	102.2	103.0
$O_2N_2H_6$/deg	104.1	103.1	101.8	103.0
$H_5N_2H_6$/deg	105.5	104.7	106.0	105.0
$O_1N_1\cdots H_4$/deg	102.8	90.9		
$O_1N_1\cdots H_6$/deg			99.4	
$O_2H_4\cdots N_1$/deg	157.0	139.9		
$N_2H_6\cdots N_1$/deg			148.0	
$H_4O_2\cdots H_1$/deg		69.7	112.7	
$O_1H_1\cdots O_2$/deg		139.1	163.9	
$N_2O_2\cdots H_1$/deg		107.5	105.2	
$O_1N_1H_4O_2$[c]/deg		3.7		
$N_1H_4O_2N_2$[c]/deg		101.5		
$N_1O_1H_1O_2$[c]/deg			7.4	
$O_1H_1O_2N_2$[c]/deg			0.7	
$H_1O_2N_2H_5$[c]/deg			116.5	
$H_1O_2N_2H_6$[c]/deg			7.1	
$H_4O_2N_2H_6$[c]/deg			124.6	
$H_1O_1N_1H_6$[c]/deg			3.6	
μ/D[d]	0.0	1.1071	1.5661	
A/GHz	12.7183583	14.9884401	12.7561841	
B/GHz	3.6169775	2.9440332	3.3478402	
C/GHz	2.9014417	2.8451005	2.7278710	

[a] see Fig. 1 for numbering of atoms
[b] see Ref. [29]
[c] dihedral angle
[d] $1\ D \equiv 3.33564 \times 10^{-30}\ C\ m$

calculations and, coupled with the use of the superior MP2 level of theory [13], enabled us to produce computed results agreeing with the experimental parameters, in most cases, within a few percent [1, 6, 11, 12, 29]. All the calculations reported here were carried out with the GAUSSIAN-86 and GAUSSIAN-88 programs, at the MP2 level with the 6-31G** basis set. Further details of our

computational procedures may be found in our previous publications [1, 6, 11, 12, 29].

3. Results and discussion

3.1. Molecular structures

The fully optimized geometrical parameters of dimer structures **I**, **III**, and **IV**, computed at the MP2/6-31G** level of theory, are presented in Table 1. The corresponding parameters of the hydroxylamine monomer, calculated at the same level [29], are included for comparison. The atom numbers refer to the structures shown in Fig. 1. In all three dimers the bond lengths and angles of the hydroxylamine molecules are only slightly perturbed from their monomer values, except when the OH or NH bonds are involved in hydrogen bonding, in which case these bonds undergo the expected increases in length. Thus the O_1H_1 bond length of dimer **I** increases by 1.5 pm, and the O_2H_4 bond length of dimer **III** by 1.4 pm. In only one dimer (**IV**) is an NH bond involved in hydrogen bonding, and this bond is predicted to increase in length by 0.5 pm, compared with the corresponding monomer value. It is interesting to note that, while all the NO bond lengths in the dimers are equal to that of the monomer, within 0.6 pm, the N_2O_2 bond length in dimer **IV**, which is adjacent to the hydrogen-bonded NH group, increases from 144.9 to 146.0 pm on dimer formation.

It is evident from the dihedral angles of dimers **III** and **IV** that, although the rings containing the hydrogen bonds are puckered, the deviations from planarity are not great. The AH···B hydrogen bond fragment which has a bond angle closest to the ideal 180° value is the $O_1H_1\cdots O_2$ bond in dimer **IV**, which is calculated to be 163.9°. It is significant that the corresponding hydrogen bond length of 188.9 pm in this dimer is the shortest among all three dimers. Dimer **III**, which contains a cyclic five-membered ring, rather than a six-membered ring as in dimer **IV**, has an $O_1H_1\cdots O_2$ hydrogen bond angle which, predictably, deviates more from linearity (139.1°), while the corresponding hydrogen bond length is greater (202.9 pm), compared with dimer **IV**. Comparison of the OH···N hydrogen bonds in the cyclic C_{2h} dimer and in dimer **III** shows the same trends, i.e. the more the hydrogen bond angle decreases the longer the corresponding hydrogen bond becomes. On the other hand, the OH···O and OH···N hydrogen bonds in dimer **III** have practically the same bond angle (131.1 and 131.9° respectively), but the N···H distance is significantly shorter (194.5 pm) than that of the O···H bond (202.9 pm). In contrast, the weakest hydrogen bond, based on its bond length, is the NH···N bond in dimer **IV**.

For the benefit of those microwave spectroscopists who might be inspired to initiate a search for the spectrum of the hydroxylamine dimer in the gas phase, we include in Table 1 the computed dipole moments and rotational constants of the three species studied here.

3.2. Hydrogen bond energies

Table 2 shows the uncorrected dimerization energies of the three cyclic hydroxylamine dimers calculated using the MP2/6-31G** theoretical model. These energies were corrected for basis set superposition error (BSSE) [30] using the

Table 2. Hydrogen bond energies, basis set superposition errors and zero-point energy differences of the hydroxylamine dimers, calculated at the MP2/6-31G** level of theory

Dimer[a]	Energy/kJ mol^{-1}			
	ΔE (uncorrected)	BSSE	ΔE°_{vib}	ΔE (corrected)
I	−59.8	13.4	10.9	−35.5
III	−42.8	17.2	9.4	−16.2
IV	−44.0	14.0	9.0	−21.0

[a] see Fig. 1

full counterpoise procedure of Boys and Bernardi [31], as we have described earlier [24]. The BSSEs are also included in Table 2. In addition, we have calculated the zero-point energy differences between the monomers and dimers, and the table also includes the dimerization energies corrected for these two effects. As can be seen, the two six-membered ring dimers (**I** and **IV**) are predicted to be more stable than the five-membered ring species (**III**), as would be expected, based on the relief of ring strain in the larger cyclic structures. The BSSEs range between 22% of the dimerization energy in the case of structure **I** to 40% in the case of dimer **III**. The most stable configuration for the hydroxylamine dimer is the centrosymmetric, C_{2h} six-membered cyclic structure, which is predicted to be more than 14 kJ mol^{-1} more stable than the asymmetric structure **IV**. The corrected mean hydrogen bond energies of dimers **I**, **III** and **IV**, at the MP2 level, are 17.75, 8.1 and 10.5 kJ mol^{-1} respectively. These results are consistent with the known stronger basic properties and poorer proton-donating properties of the amino compared with the hydroxyl group.

3.3. Vibrational wavenumbers and intensities

The predicted infrared spectra of the three hydroxylamine dimers, as represented by structures **I**, **III** and **IV** in Fig. 1, computed at the MP2/6-31G** level of theory, are summarized in Tables 3 to 5. The normal modes of vibration of the C_{2h} dimer (**I**) transform as

$$\Gamma_{vib} = 8a_g + 5a_u + 4b_g + 7b_u,$$

while those of dimers **III** and **IV**, which belong the C_1 point group, are all of symmetry *a*.

Structure I. The centrosymmetric structure of the six-membered cyclic dimer, **I**, ensures that each normal mode of vibration of this species is composed of equal contributions from the vibrations of each monomer unit. Most of the intramolecular vibrations of the dimer can be correlated with normal modes of the hydroxylamine monomer, as is evident from the descriptions of the dimer modes in Table 3. The torsional mode of the monomer, ν_9, however, appears to have no direct counterpart in the dimer. An analysis of the predicted monomer torsional mode [29] shows that the vibration consists of the coupling of an out-of-plane displacement of the hydroxyl hydrogen atom and a counter out-of-plane rocking motion of the amino NH_2 group, the contributions being approximately 68 and 32%, respectively. Formation of the hydrogen bonded ring perturbs the torsional

Table 3. The predicted infrared spectrum, at the MP2/6-31G** level, of the C_{2h} six-membered cyclic hydroxylamine dimer **I**[a]

Symmetry species	Mode	Approximate description	$\tilde{\nu}/cm^{-1}$	A/km mol^{-1}
a_g	ν_1	ν_s(OH)	3570	—
	ν_2	$\nu_{ss}(NH_2)$	3524	—
	ν_3	$\delta_s(NH_2)$	1702	—
	ν_4	δ_s(NOH)	1613	—
	ν_5	$w(NH_2)$	1206	—
	ν_6	ν_s(NO)	978	—
	ν_7	δ_s(OH···N)	248	—
	ν_8	ν_s(H···N)	215	—
a_u	ν_9	$\nu_{aa}(NH_2)$	3629	1.6
	ν_{10}	$tw(NH_2)$	1324	0.17
	ν_{11}	γ_s(OH···N)	854	253
	ν_{12}	$r(NH_2)$	225	17
	ν_{13}	$r(NH_2)$	79	24
b_g	ν_{14}	$\nu_{aa}(NH_2)$	3629	—
	ν_{15}	$tw(NH_2)$	1330	—
	ν_{16}	γ_a(OH···N)	718	—
	ν_{17}	$r(NH_2)$	315	—
b_u	ν_{18}	ν_a(OH)	3618	1006
	ν_{19}	$\nu_{ss}(NH_2)$	3529	2.5
	ν_{20}	$\delta_a(NH_2)$	1699	39
	ν_{21}	δ_a(NOH)	1550	82
	ν_{22}	$w(NH_2)$	1236	230
	ν_{23}	ν_a(NO)	970	9.6
	ν_{24}	δ_a(OH···N)	254	7.8

[a] see Fig. 1

vibrations of the monomer units with the result that the out-of-plane motions of the bonded hydrogen atoms appear as in-phase and out-of-phase combinations in the intermolecular modes ν_{11} and ν_{16}, which have counterparts in the water and ammonia dimers discussed previously [1], and which are calculated to lie at much higher wavenumbers than the monomer torsional mode. In the complex of hydroxylamine with water [11], which also has a cyclic structure, the counterpart of the monomer torsional mode is described as a coupling of the out-of-plane bending of the OH···O group with the HOH-twisting motion of the water unit, and appears at 690 cm^{-1}. In the hydroxylamine-ammonia complex [12], which is more linear in nature, the NOH torsional motion is calculated to appear at 814 cm^{-1}. The blue shifts experienced by this mode in each of these complexes are directly proportional to the calculated mean hydrogen bond energies [11, 12]; thus the greater the strength of interaction the larger the blue shift in the wavenumber of the torsional mode in the complex. The rocking motions of the amino NH_2 groups are recognizable as modes ν_{12} and ν_{17} in the dimer, but since the hydrogen atoms are not directly involved in the ring, these vibrations appear at very low wavenumbers and the infrared active mode, ν_{12}, is of low intensity.

Structure III. In the case of the five-membered cyclic dimer (**III**), due to its asymmetric nature, most of the intramolecular normal modes are largely centred in one monomer unit or the other (A or B, see Fig. 1), and may be compared directly with the corresponding modes of the monomer. Three exceptions to this

Table 4. The predicted infrared spectrum, at the MP2/6-31G** level, of the C_1 five-membered cyclic hydroxylamine dimer **III**[a]

Mode	Approximate description[b]	$\tilde{\nu}$/cm^{-1}	A/km mol^{-1}
ν_1	ν(OH)(A)	3772	293
ν_2	ν_a(NH_2)(A)	3642	1.8
ν_3	ν_a(NH_2)(B)	3632	2.6
ν_4	ν(OH)(B)	3628	254
ν_5	ν_s(NH_2)(A)	3537	2.3
ν_6	ν_s(NH_2)(B)	3527	6.5
ν_7	δ(NH_2)(B)	1706	17
ν_8	δ(NH_2)(A)	1698	17
ν_9	δ(NOH)(A)(64) + δ(NOH)(B)(34)OP)	1538	35
ν_{10}	δ(NOH)(B)(67) + δ(NOH)(A)(33)(IP)	1514	44
ν_{11}	tw(NH_2)(B)	1349	0.72
ν_{12}	tw(NH_2)(A)	1331	0.17
ν_{13}	w(NH_2)(B)	1217	139
ν_{14}	w(NH_2)(A)	1206	155
ν_{15}	ν(NO)(A)(84) + δ(OH···N)(16)	970	17
ν_{16}	ν(NO)(B)	954	13
ν_{17}	δ(OH···N)	846	233
ν_{18}	γ(OH···O)	617	114
ν_{19}	r(NH_2)(A)	319	7.8
ν_{20}	ν(H···N)	257	39
ν_{21}	ν(H···O)	207	14
ν_{22}	r(NH_2)(B)	136	17
ν_{23}	r(NH_2)(A)(59) + δ(ONH)(B)(17)	107	11
ν_{24}	r(NH_2)(B)(57) + δ(ONH)(A)(17)	54	0.29

[a] see Fig. 1

[b] Numbers in parentheses indicate major percentage contributions (>10%) of localized modes to each normal mode; A and B refer to the identifications of the monomer units shown in Fig. 1; IP – in-phase, OP – out-of-phase

statement are apparent from the descriptions in Table 4. The NOH-bending modes, ν_9 and ν_{10}, of the two monomer units are strongly coupled, with each monomer, in turn, contributing about twice that of the other to the displacements of the dimer. Furthermore, the NO bond of monomer A, unlike that of monomer B, forms part of the ring structure, and the stretching mode of this bond, ν_{15}, induces a displacement of the bonded hydrogen atom, H_4, of monomer B (see Fig. 1). As discussed above for the C_{2h} dimer, the involvement of both hydroxyl hydrogen atoms in the ring structure again perturbs the torsional vibrations, with the consequent appearance of two low frequency NH_2-rocking vibrations (ν_{19} and ν_{22}).

Structure IV. The formation of the NH···N hydrogen bond in the six-membered C_1 ring dimer (**IV**), as illustrated in Fig. 1, disturbs the local C_s symmetry of monomer B, in particular that of the NH_2 group. Consequently, the symmetric and antisymmetric NH_2-stretching modes (ν_4 and ν_6) are partly decoupled and are best described in terms of the separate stretching vibrations of the bonded (b) and free (f) NH bonds. The same effect is evident in the vibrational modes which correspond to the bending, twisting and wagging motions of the amino group (ν_7, ν_{10}, ν_{11}, ν_{13} and ν_{14}). For convenience, the descriptions "bending", "twisting"

Table 5. The predicted infrared spectrum, at the MP2/6-31G** level, of the C_1 six-membered cyclic hydroxylamine dimer **IV**[a]

Mode	Approximate description[b]	$\tilde{\nu}$/cm^{-1}	A/km mol^{-1}
ν_1	ν(OH)(B)(f)	3885	46
ν_2	ν(OH)(A)(b)	3730	385
ν_3	ν_a(NH$_2$)(A)	3626	0.07
ν_4	ν(NH)(f)(77) + ν(NH)(b)(23)(OP)	3618	18
ν_5	ν_s(NH$_2$)(A)	3525	3.5
ν_6	ν(NH)(b)(75) + ν(NH)(f)(24)(IP)	3489	75
ν_7	δ(ONH)(b)(57) + δ(ONH)(f)(40)	1727	15
ν_8	δ(NH$_2$)(A)	1701	16
ν_9	δ(NOH)(A)	1552	31
ν_{10}	δ(NOH)(B)(44) + δ(ONH)(b)(44)	1424	20
ν_{11}	tw(NH$_2$)(B)	1393	11
ν_{12}	tw(NH$_2$)(A)	1334	0.32
ν_{13}	w(NH$_2$)(B)(72) + w(NH$_2$)(A)(28)	1228	263
ν_{14}	w(NH$_2$)(A)(68) + w(NH$_2$)(B)(32)	1213	18
ν_{15}	ν(NO)(A)	967	5.3
ν_{16}	ν(NO)(B)	939	14
ν_{17}	γ(OH···O)	702	170
ν_{18}	τ(NO)(B)(84) + γ(OH···O)(16)	447	146
ν_{19}	r(NH$_2$)(A)(43) + τ(OH)(B)(28) + τ(NH)(f)(16) + γ(NH···N)(13)	332	14
ν_{20}	ν(H···O)	225	4.6
ν_{21}	r(NH$_2$)(A)(36) + τ(NH)(f)(22) + τ(OH)(B)(18) + δ(NH···N)(15)	198	7.9
ν_{22}	r(NH$_2$)(A)(54) + δ(NH···N)(18)	195	10
ν_{23}	ν(H···N)(43) + tw(NH$_2$)(A)(39)	178	0.48
ν_{24}	r(NH$_2$)(A)(33) + τ(NH)(f)(25) + τ(OH)(17)	64	5.1

[a] see Fig. 1

[b] Numbers in parentheses indicate major percentage contributions (>10%) of localized modes to each normal mode; A and B refer to the identifications of the monomer units shown in Fig. 1; IP – in-phase, OP – out-of-phase; f – free, b – bonded

and "wagging" have been retained, although the motions of the NH bonds of unit B are not equivalent. This is reflected in the unequal percentage contributions of each bond to the dimer modes ν_4, ν_6, ν_7 and ν_{10}, as shown in Table 5. It is interesting to note that in this dimer, monomer unit B, which contains the non-bonded OH bond, exhibits a vibration (ν_{18}) which has a form, and a predicted wavenumber (447 cm^{-1}) which closely resemble those calculated for the torsional mode of the hydroxylamine momomer (408 cm^{-1}) [29].

3.4. Comparison of calculated wavenumbers and intensities of dimers and monomers

The shifts in the infrared wavenumbers, and the changes in the values of the intensities of the hydroxylamine monomer bands which occur on formation of the three dimers, have been calculated, and are presented in Table 6. Owing to the wide variation in the calculated positions of the torsional vibrations of the

Table 6. Calculated monomer-dimer wavenumber shifts and intensity ratios of the hydroxylamine dimers

Parent monomer mode	Dimer								
	I			III			IV		
	Dimer mode	$\Delta\tilde{\nu}$/ cm^{-1}	$A_{dimer}/A_{monomer}$	Dimer mode	$\Delta\tilde{\nu}$/ cm^{-1}	$A_{dimer}/A_{monomer}$	Dimer mode	$\Delta\tilde{\nu}$/ cm^{-1}	$A_{dimer}/A_{monomer}$
ν_1	ν_1	−322	—	ν_1	−120	8.5	ν_1	−7	1.3
	ν_{18}	−274	29.2	ν_4	−264	7.4	ν_2	−162	11.2
ν_7	ν_9	−7	(40)	ν_2	6	(45)	ν_3	−10	(2)
	ν_{14}	−7	—	ν_3	−4	(65)	ν_4	−18	(450)
ν_2	ν_2	−7	—	ν_5	6	(2)	ν_5	−6	(2)
	ν_{19}	−2	(2)	ν_6	−4	(4)	ν_6	−42	(48)
ν_3	ν_3	−2	—	ν_7	2	0.91	ν_7	23	0.81
	ν_{20}	−5	2.1	ν_8	−6	0.91	ν_8	−3	0.86
ν_4	ν_4	183	—	ν_9	108	1.6	ν_9	122	1.4
	ν_{21}	120	3.8	ν_{10}	84	2.0	ν_{10}	−6	0.93
ν_8	ν_{10}	−23	(43)	ν_{11}	2	(180)	ν_{11}	46	(2750)
	ν_{15}	−17	—	ν_{12}	−16	(43)	ν_{12}	−13	(80)
ν_5	ν_5	14	—	ν_{13}	25	0.89	ν_{13}	36	1.7
	ν_{22}	44	1.5	ν_{14}	14	1.0	ν_{14}	21	0.01
ν_6	ν_6	24	—	ν_{15}	16	1.7	ν_{15}	13	0.50
	ν_{23}	16	0.95	ν_{16}	0	1.3	ν_{16}	−15	1.4

various dimers, referred to above, resulting from the forms of those vibrations not being directly comparable with that of the monomer, we have not calculated any wavenumber shifts relative to the monomer mode ν_9. Moreover, the NH_2-stretching and twisting modes of the hydroxylamine monomer (ν_2, ν_7 and ν_8) are calculated to be very weak [29]. Consequently, even modest increases in intensity of the corresponding dimer modes result in intensity ratios which may be artificially high. These ratios have been placed in parentheses in Table 6, to indicate that they are not regarded as significant.

The main features of the results presented in Table 6 are the predicted red shifts and intensity enhancements of the infrared bands of the hydrogen-bonded OH- and NH-stretching vibrations of the dimers. The largest calculated shifts occur in the OH-stretching vibrations of the cyclic C_{2h} dimer (**I**), and the infrared active mode, ν_{18}, is also predicted to undergo the largest genuine intensity enhancement. If a comparison is made between mode ν_{18} of dimer **I** and mode ν_4 of dimer **III**, both of which are OH-stretching vibrations of OH bonds involved in similar OH···N hydrogen-bonded interactions, it can be seen that the predicted shifts are very similar (274 and 264 cm^{-1} respectively), as are the hydrogen bond lengths (191.4 and 194.5 pm respectively) (see Table 1). The magnitudes of the wavenumber shifts are indicative of the relatively strong OH···N hydrogen-bonded interaction [32].

Modes ν_1 of dimer **III** and ν_2 of dimer **IV** may also be compared, since both these vibrations arise from the OH-stretching motions in similar OH···O hydrogen bonds. Mode ν_1 is calculated to shift by 120 cm^{-1}, compared with the monomer value, while the shift in mode ν_2 is 162 cm^{-1}. The difference between these two shifts is probably due to the fact that the $O_2 \cdots H_1$ hydrogen bond

length in dimer **IV** is shorter (188.9 versus 202.9 pm) and the $O_1H_1\cdots O_2$ hydrogen bond angle is closer to linearity (163.9 versus 139.1°) than the corresponding values in dimer **III**. The hydrogen bond in the five-membered dimer is thus expected to be weaker and the corresponding wavenumber shift is consequently smaller [32].

Dimer **IV** is the only structure with an NH···N hydrogen bond, and modes ν_4 and ν_6 of this dimer both involve the stretching of the bonded NH bond (see Table 5). Of these two modes, ν_6 has the larger contribution from the bonded NH-stretching vibration, and it also has the larger predicted shift. Compared with the shifts in the bonded OH-stretching wavenumbers, this relatively small shift (42 cm^{-1}) is typical of a rather weak NH···N interaction [32], consistent with the poor proton-donating properties of the amino NH_2 group. The weak interaction is also reflected in the fact that the H···N hydrogen bond length (218.3 pm) is the longest of any of the hydrogen bonds in all three dimers (see Table 1).

Although the extent of deviation of the hydrogen bond angle from the ideal 180° is clearly important for the strength of hydrogen bonding, the results presented above indicate that the order of decreasing hydrogen bond strength in the hydroxylamine dimers is OH···N > OH···O > NH···N. This observation is consistent with the fact that the linear water dimer is predicted to have a higher dimerization energy than the corresponding linear ammonia dimer (19.6 versus 12.5 kJ mol^{-1}) [1], and that the cyclic C_{2h} hydroxylamine dimer is predicted to be the most stable configuration of the three considered here (see Table 2). Dimer **IV** has an NH···N interaction which is predicted to be weak, but because of the six-membered ring structure, the OH···O geometry is more favourable than that in dimer **III**, and this would seem to be sufficient to make dimer **IV** the more stable structure of the two.

It is also evident from the results given in Table 6 that the hydrogen-bonded NOH-bending modes are shifted to higher frequency. The calculated blue shifts (excluding the infrared inactive mode of dimer **I**) are fairly similar, ranging from 84 cm^{-1} for the ν_{10} mode of dimer **III** to 122 cm^{-1} for the ν_9 mode of dimer **IV**. The twisting vibration of the NH_2 group of monomer **B** in dimer **IV**, ν_{11}, effectively involves a bending of the ONH bond angle which forms part of the NH···N fragment, and hence, as can be seen in Table 6, it is also predicted to shift 46 cm^{-1} to higher wavenumber. Apart from ν_{11} of dimer **III**, the other twisting vibrations of the three dimers are found at slightly lower wavenumbers than that of the monomer [29].

3.5. Comparison of calculated with experimental wavenumbers

Table 7 lists the positions of the bands observed in the infrared spectra of hydroxylamine trapped in nitrogen matrices at 17 K, and assigned to vibrational modes of dimeric species [5]. This table also shows the closest match to the observed wavenumbers of each of the calculated wavenumbers of the infrared active modes of the three dimers, without prejudice to the correct dimer structure, along with the calculated/experimental wavenumber ratios for each mode. Since, in the case of the centrosymmetric dimer (**I**) there are only twelve expected infrared active modes, and of these, three are expected to absorb below our lower wavenumber limit of 250 cm^{-1}, the observation of only nine absorptions having concentration and warm-up behaviour consistent with their assign-

Table 7. Comparison of calculated wavenumbers for the three hydroxylamine dimers with experimental wavenumbers observed in nitrogen matrices

	Dimer					
	I		**III**		**IV**	
$\tilde{\nu}$(expt)/ cm^{-1a}	Assignment	$\tilde{\nu}$(calc)/ cm^{-1b}	Assignment	$\tilde{\nu}$(calc)/ cm^{-1b}	Assignment	$\tilde{\nu}$(calc)/ cm^{-1b}
3444	ν_9	3629 (1.05)	ν_2	3642 (1.06)	ν_4	3618 (1.05)
			ν_3	3632 (1.05)		
3346	ν_{18}	3618 (1.08)	ν_1	3772 (1.13)	ν_2	3730 (1.11)
3302			ν_4	3628 (1.10)		
3290					ν_6	3489 (1.06)
1623	ν_{20}	1699 (1.05)	ν_7	1706 (1.05)	ν_7	1727 (1.06)
			ν_8	1698 (1.05)		
1472	ν_{21}	1550 (1.05)	ν_9	1538 (1.04)	ν_9	1552 (1.05)
1452			ν_{10}	1514 (1.04)		
1290	ν_{10}	1324 (1.03)	ν_{11}	1349 (1.05)	ν_{11}	1393 (1.08)
			ν_{12}	1331 (1.03)	ν_{12}	1334 (1.03)
1165	ν_{22}	1236 (1.06)	ν_{13}	1217 (1.04)	ν_{13}	1228 (1.05)
1158			ν_{14}	1206 (1.04)	ν_{14}	1213 (1.05)
904	ν_{23}	970 (1.07)	ν_{15}	970 (1.07)	ν_{15}	967 (1.07)
885					ν_{16}	939 (1.06)
761	ν_{11}	854 (1.12)	ν_{17}	846 (1.11)	ν_{17}	702 (0.92)
564			ν_{18}	617 (1.09)		
449					ν_{18}	447 (1.00)
268	ν_{24}	254 (0.95)	ν_{20}	257 (0.96)	ν_{20}	225 (0.84)
(absolute mean)		1.06		1.06		1.07

[a] see Ref. [5]

[b] numbers in parentheses are the calculated/experimental wavenumber ratios for each mode

ment to dimers was a relatively simple matter. The assignments to modes ν_{11}, ν_{18} and ν_{22} were fairly straightforward, since these modes were predicted to have substantial intensities (see Table 3), and would therefore have fairly high probabilities of being detected, even at fairly low concentrations. Modes ν_{20} and ν_{21}, having intermediate intensities, are also assigned with some confidence. However, the assignments of modes ν_9, ν_{10}, ν_{23} and ν_{24}, which are expected to be very weak, are more tenuous, while ν_{12} and ν_{13} are probably outside our observable wavenumber range. The computed wavenumbers may be fitted to the observed with an average error of 99 cm^{-1}, or 6.36%.

In the case of dimer **III**, we have been able to locate thirteen bands which may reasonably be assigned to the eighteen modes of the dimer which appear in the experimental wavenumber range. In the OH- and NH-stretching region, the assignment of the strong, broad OH bands is unambiguous, although the wavenumber of the higher frequency band of the two, that engaged in the weaker OH···O interaction, is severely overestimated by the calculation. This leads to a calculated/experimental ratio of 1.13 for this mode, significantly higher than the average extent of overestimation. Of the vibrations in this region, only the bonded OH-stretching vibrations have high intensities, while the NH_2-stretching modes are very weak, and their assignments have lower confidence levels. The dimer modes ν_7, ν_8, ν_{11} and ν_{12} occur in closely separated pairs, being the

individual vibrations of monomer units A and B, which are highly uncoupled. Moreover, the individual members of each pair have fairly similar calculated intensities, therefore it is difficult to choose the more likely candidate for assignment from each pair, and the assignments for these modes in Table 7 are consequently bracketed together. The intermolecular modes, ν_{17} and ν_{18}, have rather higher calculated/experimental wavenumber ratios than the intramolecular vibrations, as we found for ν_{11} of dimer **I**, and also for $(H_2O)_2$, $(NH_3)_2$ [1], $HOH{\cdot}NH_3$ [6, 33] and $NH_2OH{\cdot}NH_3$ [12, 34]. The overall mean error is 115 cm^{-1}, or 6.30%.

Dimer **IV** is predicted to have four relatively intense modes, the bonded OH-stretching (ν_2), the combination of the NH_2-wagging modes of monomers A and B (ν_{13}), the out-of-plane OH···O hydrogen bond bending mode (ν_{17}) and the torsional vibration about the NO bond of unit B (ν_{18}). These may be readily assigned, although the calculated wavenumber of ν_{17} is, unusually, lower than the experimental value. The same is true of ν_{20}, the H···O hydrogen bond stretching vibration. Most of the remaining modes have reasonably high intensities, and the relevant assignments are expected to be fairly accurate. The ν_{12} and ν_{15} vibrations, however, are predicted to be very weak and the assignments to these modes must be regarded as hopeful, at best. The computed wavenumber of the bonded OH-stretching band (ν_2) is excessively high, as found for dimer **III**, and this, together with the appearance of two wavenumbers calculated to be actually lower than the experimental values, weakens the case for dimer **IV** being the correct structure, even though the mean wavenumber error (102 cm^{-1}) and the mean absolute percentage error (6.93%) are almost indistinguishable from those of dimer **I**. The more consistent agreement between the computed values for dimer **I** and the experimental wavenumbers of the hydroxylamine dimer suggests that dimer **I** is the preferred structure. This observation, taken together with the larger computed dimerization energy for this species, compared with those of the two alternative structures considered here (see Table 2), convinces us that the most likely structure of the hydroxylamine dimer is the centrosymmetric, C_{2h}, doubly OH···N hydrogen-bonded form.

Acknowledgments. T.A.F. acknowledges the financial support of the Foundation for Research Development, and G.A.Y. thanks the University of the Witwatersrand for the award of a Backeberg Scholarship for 1988 and 1989.

References

1. Yeo GA, Ford TA Struct Chem (in press)
2. Del Bene JE (1972) J Chem Phys 57:1899
3. Yeo GA, Ford TA (1989) J Mol Structure (Theochem) 200:507
4. Withnall R, Andrews L (1988) J Phys Chem 92:2155
5. Yeo GA, Ford TA (1990) J Mol Structure 217:307
6. Yeo GA, Ford TA (1991) Can J Chem 69:632
7. Hehre WJ, Stewart RF, Pople JA (1969) J Chem Phys 51:2657
8. Ditchfield R, Hehre WJ, Pople JA (1971) J Chem Phys 54:724
9. Francl MM, Pietro WJ, Hehre WJ, Binkley JS, Gordon MS, DeFrees DJ, Pople JA (1982) J Chem Phys 77:3654
10. McIver JW (1974) Accounts Chem Research 7:72
11. Yeo GA, Ford TA J Mol Structure (Theochem) (in press)
12. Yeo GA, Ford TA (1991) Chem Phys Letters 178:266

13. Møller C, Plesset MS (1934) Phys Rev 46:618
14. Binkley JS, Whiteside RA, Hariharan PC, Seeger R, Pople JA, Hehre WJ, Newton MD (1978) QCPE 10:368
15. Cook CM (1981) QCPE 13:391
16. Binkley JS, Whiteside RA, Krishnan R, Seeger R, DeFrees DJ, Schlegel HB, Topiol S, Kahn LR, Pople JA (1980) QCPE 13:406
17. Foley CK, Chesnut DB (1985) QCPE Bull 5:99
18. Chin S, Ford TA, Person WB (1984) J Mol Structure 113:341
19. Chin S, Ford TA (1985) J Mol Structure (Theochem) 133:193
20. Yeo GA, Ford TA (1986) J Mol Structure 141:331
21. Yeo GA, Ford TA (1986) S Afr J Chem 39:243
22. Chin S, Ford TA (1987) J Mol Structure (Theochem) 152:363
23. O'Neill FMM, Yeo GA, Ford TA (1988) J Mol Structure 173:337
24. Yeo GA, Ford TA (1988) J Mol Structure (Theochem) 168:247
25. Bräsler MJ, Carr VCE, Gerazounis MG, Jugga NR, Yeo GA, Ford TA (1988) J Mol Structure (Theochem) 180:241
26. Evans DG, Yeo GA, Ford TA (1988) Faraday Disc Chem Soc no. 86:55
27. Frisch MJ, Binkley JS, Schlegel HB, Raghavachari K, Melius CF, Martin RL, Stewart JJP, Bobrowicz FW, Rohlfing CM, Kahn LR, DeFrees DJ, Seeger R, Whiteside RA, Fox DJ, Fleuder EM, Pople JA (1984) GAUSSIAN-86. Carnegie-Mellon Quantum Chemistry Publishing Unit, Pittsburgh, PA 15213
28. Frisch MJ, Head-Gordon M, Schlegel HB, Raghavachari K, Binkley JS, Gonzalez C, DeFrees DJ, Fox DJ, Whiteside RA, Seeger R, Melius CF, Baker J, Martin R, Kahn LR, Stewart JJP, Fleuder EM, Topiol S, Pople JA (1988) GAUSSIAN-88. Gaussian Inc, Pittsburgh, PA 15213
29. Yeo GA, Ford TA (1990) J Chem Soc Faraday Trans 86:3067
30. Kestner NR (1968) J Chem Phys 48:252
31. Boys SF, Bernardi F (1970) Mol Phys 19:553
32. Hadzi D, Bratos S (1976) In: Schuster P, Zundel G, Sandorfy C (eds) The hydrogen bond, vol. II, North-Holland, Amsterdam, pp 565–611
33. Yeo GA, Ford TA (1991) Spectrochim Acta Part A 47:485
34. Yeo GA, Ford TA (1992) Spectrochim Acta Part A (in press)